Revealing Light-Induced Charge Density Wave Melting and Carrier Redistribution in 1T-$TiSe_2$

Wanying Chen(陈婉莹)[1†], Haoyuan Zhong(钟浩源)[1†], Changhua Bao(鲍昌华)[1], Fei Wang(王飞)[1], Xuanxi Cai(蔡轩羲)[1], Chenxia Yun(运晨霞)[2], Hao Teng(滕浩)[2], Zhiyi Wei(魏志义)[2], and Shuyun Zhou(周树云)[1,3*]

[1]*State Key Laboratory of Low-Dimensional Quantum Physics and Department of Physics, Tsinghua University, Beijing 100084, China*
[2]*Beijing National Laboratory for Condensed Matter Physics, Institute of Physics, Chinese Academy of Sciences, Beijing 100190, China*
[3]*Frontier Science Center for Quantum Information, Beijing 100084, China*

(Received 9 October 2024; accepted manuscript online 26 November 2024)

Capturing ultrafast dynamics over a large momentum space is critical for revealing the relationship between the electronic and structural modulations in quantum materials. Here, by performing time- and angle-resolved photoemission spectroscopy measurements at the Synergetic Extreme Condition User Facility (SECUF) equipped with an extreme ultraviolet light source, we reveal the ultrafast dynamics of a charge-density wave (CDW) material, 1T-$TiSe_2$, upon photoexcitation. Pump-induced CDW melting is revealed from two aspects: gap closing of the CDW at the Brillouin zone (BZ) center and weakening of the CDW folded band at the BZ boundary. By comparing the transient electronic structure and spectral weight over a large momentum space, we further reveal the carrier redistribution involving the excitation of electrons from the Γ point to the M point. This study provides a comprehensive picture of the physics and ultrafast dynamics of a CDW material across the entire BZ.

DOI: 10.1088/0256-307X/42/1/017101 CSTR: 32039.14.0256-307X.42.1.017101

1. Introduction. Novel macroscopic phenomena in many solid-state materials involve the displacement of electrons by a large momentum space that sometimes spans from the center of the first Brillouin zone (BZ) to its boundary. When combined with ultrafast laser pulses, such collective electronic states can be probed and manipulated, resulting in exotic quantum properties such as light-driven Floquet states,[1–5] light-induced superconductivity[6,7] and the photoinduced emergence of metastable states.[8–11] A typical and intriguing example is the charge density wave (CDW), in which electrons in different momentum spaces are coupled via the CDW wave vector, providing a suitable platform for optical manipulation.[12–17] The layered transition metal dichalcogenide 1T-$TiSe_2$ exhibits interesting CDW phases,[18] giving birth to a broad variety of many-body interactions, including electron-electron[19–22] and electron-phonon interactions.[23–25] By utilizing time- and angle-resolved photoemission spectroscopy (TrARPES),[26–28] quasiparticle interactions and ultrafast carrier dynamics can be revealed using energy- and momentum-resolved information in such CDW systems.[29–32] Significant progress has been made in understanding the melting process of the long-range charge order and emerging new electronic states.[29,33–38] To date, most studies have focused on the spectral features in a specific momentum space to capture light-induced changes at ultrafast timescales. An experimental investigation of ultrafast dynamics across a large BZ is required to map the long-range order evolution and establish the interplay between electrons at the BZ center and BZ boundary.

In this study, by taking advantage of extreme ultraviolet light (XUV)-based TrARPES, we reveal the ultrafast dynamics of light-induced CDW melting, together with carrier redistribution, in 1T-$TiSe_2$ [see the schematic in Fig. 1(a)]. The CDW melting dynamics are revealed in two ways. First, near the BZ center (Γ point), the upshift of the Se_{4p} band after pumping indicates the CDW gap closing. Second, near the BZ boundary (point M), the weakening of the CDW folded band is observed. In particular, the distinctive spectral weight transfer of large momentum indicates that the CDW phase strongly modifies the electronic structure. Moreover, the ultrafast nonequilibrium carrier dynamics of both the Se_{4p} and Ti_{3d} bands are captured, revealing excitation from the Γ point to the M point through electron-phonon scattering. Our work provides comprehensive insights into the CDW physics of $TiSe_2$ and demonstrates the intriguing interactions between electrons at the BZ center and those at the BZ boundary in nonequilibrium carrier dynamics.

2. Methods. TrARPES measurements were performed at the attosecond dynamics experimental station

†These authors contributed equally to this work.
*Corresponding author. Email: syzhou@mail.tsinghua.edu.cn
© 2025 Chinese Physical Society and IOP Publishing Ltd. All rights, including for text and data mining, AI training, and similar technologies, are reserved.

(D2) at the Synergetic Extreme Condition User Facility (SECUF).[39] The fundamental laser source was a Yb-doped fiber laser operating at a repetition rate of 100 kHz. The high-harmonic generation (HHG) light source in the XUV range with a photon energy of 16.8 eV allows the coverage of a large momentum range of 1.8 $Å^{-1}$. Thus, the carrier dynamics can be observed at both the Γ point and the BZ boundary. With a high photon flux of 10^{10}–10^{11} photons/s, the HHG light source provides high data acquisition efficiency to capture the dynamics at both the Γ and M points.[40,41]

3. Results and Discussion. The layered compound 1T-$TiSe_2$ exhibits a $(2\times2\times2)$ CDW structure[18] with a transition temperature of 200 K, which originates from the hybrid Jahn–Teller effect and excitonic condensation.[19,42,43] Figure 1(b) shows the experimental dispersion image measured at equilibrium in the CDW state along the Γ-M direction using a high-brightness XUV light source. It includes Se_{4p} valence bands at the Γ point (center of the BZ) and a Ti_{3d} conduction band at the M point (boundary of the BZ), which are the main components of the band structure. Below the CDW transition temperature, folded Se_{4p} bands appear at point M because of the new periodicity of the commensurate CDW in real space [indicated by the red dashed lines in Fig. 1(c)]. In the following sections, we focus on the evolution of both these bands to understand the CDW melting and ultrafast carrier transfer mechanisms.

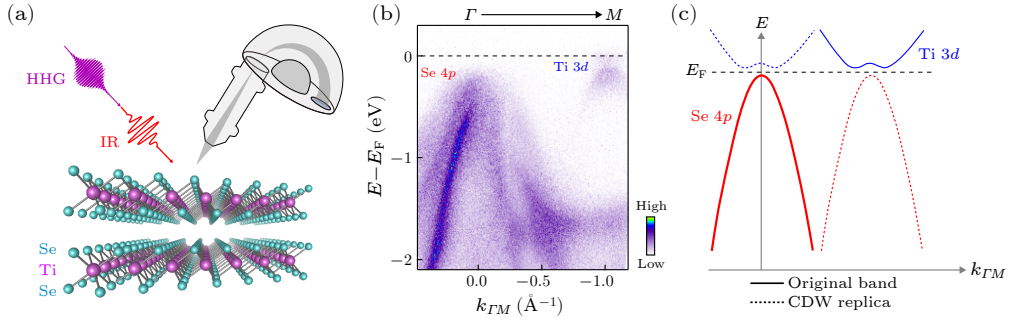

Fig. 1. Schematic of XUV TrARPES and observation of the CDW state in $TiSe_2$ at 20 K. (a) Schematic of laser-based XUV TrARPES setup. (b) Dispersion image of the CDW phase in $TiSe_2$ along the Γ-M direction without a pump. (c) Schematic of the CDW phase induced band folding in momentum space.

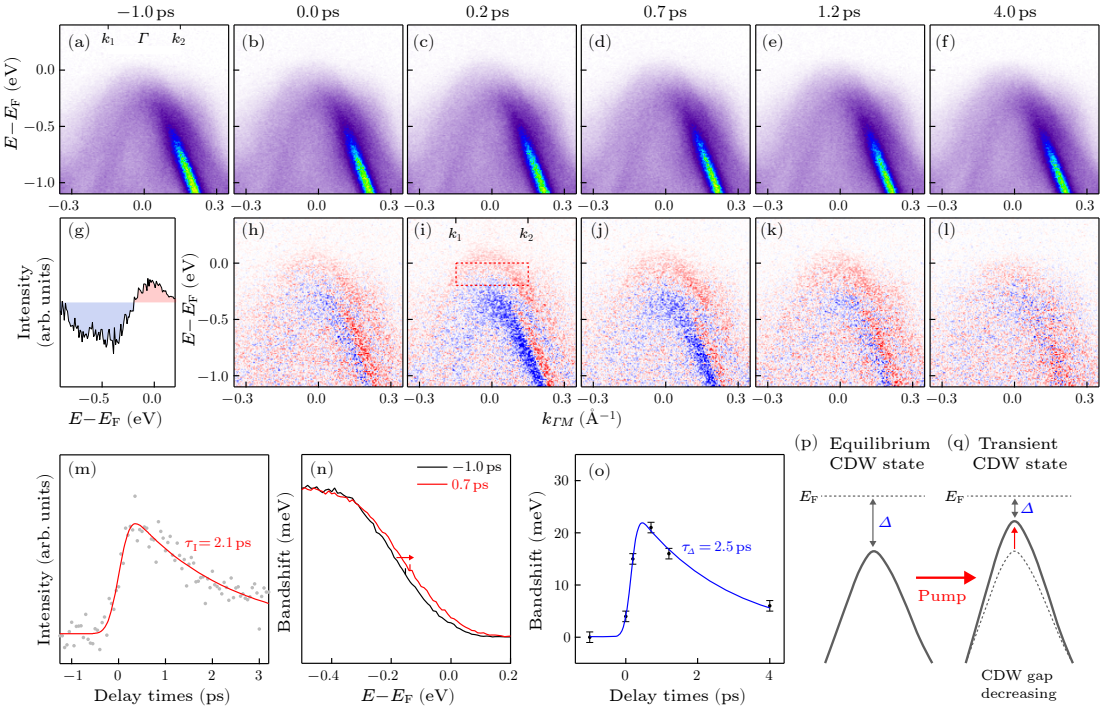

Fig. 2. Light-induced dynamics and spectral weight distribution around the BZ center. (a)–(f) TrARPES dispersion images at different delay times around the Γ point along the M-Γ-M direction. The pump photon energy was 1.2 eV and the pump fluence was 60 $\mu J/cm^2$. (g) Integrated spectral weight covering the momentum regions around the Γ point. (h)–(l) Differential TrARPES spectra at different delay times after subtracting the spectrum at −1.0 ps. (m) Intensity evolution of the band shift as a function of delay time obtained by integrating over the red box marked in (i) and fitted according to Refs. [44–46]. (n) Band shift at 0.7 ps and −1.0 ps obtained by integrating EDC from k_1 to k_2. (o) Band shift evolution as a function of delay time. (p) and (q) Schematics of the equilibrium CDW state before the pump and transient CDW state after the pump at the Γ point. The pump decreases the CDW gap.

First, we focus on the dynamics of the Se_{4p} bands at the Γ point. Figures 2(a)–2(f) show snapshots of the dispersion images measured along the M-Γ-M direction at different delay times. Upon pumping, the transiently excited states could be resolved more clearly in the differential images shown in Figs. 2(h)–2(l). The Se_{4p} bands exhibited a distinctive increase in the spectral intensity upon pumping, as shown in Figs. 2(i) and 2(j), suggesting a band shift from lower energy to higher energy. Such an upshift lasting longer than the duration of the pump laser is a signature of the light-induced perturbation of the CDW bandgap closing, which agrees with a previous study at a higher temperature of 80 K.[31] The laser-induced transient heating effect was ruled out because the highest transient lattice temperature in our experiment was estimated to be 64 K (see Supplementary Information for the calculation), which is far below the CDW transition temperature of $T_C = 200$ K. Such a small change in the transient temperature could not induce a change in the gap size of 25 meV, as observed in our experiments. To track the dynamics of the shifting Se_{4p} bands, Fig. 2(m) shows the temporal evolution of the intensity in the gap region, as indicated by the red dashed box in Fig. 2(i). The lifetime of such gap-closing features was 2.1 ± 0.2 ps, suggesting that the upshift was indeed a dynamic perturbation of the CDW and not just the thermalization of the valence band (VB) electrons. Such transient upshift can also be confirmed and extracted by fitting the integrated energy distribution curves (EDCs) from delay time k_1 to k_2 using the Fermi–Dirac distribution function, $f(E) = \frac{1}{e^{(E-E_{VB}(t))/k_b t}+1}$, where $E_{VB}(t)$ represents the VB edge position at delay time t, as shown in Figs. 2(n) and 2(o) (Supplementary Information, Fig. S1). According to calculations, our applied pump fluence of 60 μJ/cm^2 corresponds to an excitation density of 0.008 photons per Ti atom,[29] which causes a relative suppression of screening for the origin of the correlation-induced phase transitions. The CDW melting dynamics are summarized schematically in Figs. 2(p) and 2(q), where the Se_{4p} valence band at the BZ center shifts upon photo-excitation, leading to the closing of the CDW gap. Figure 2(g) shows this upshift feature, which is obtained by integrating the spectral intensity from k_1 to k_2 at Δt, as marked in Fig. 2(i). Figure 2(g) also presents an intrinsic decrease in the spectral weight distribution, regardless of the specific momentum regions (Supplementary Information Fig. S2). In addition, both valence bands showed similar upshifts after photo-excitation, which were observed off the Γ point (Supplementary Information, Fig. S3). These features confirm that there is a spectral transfer to other momenta, which will be explored later.

Following the extension of the BZ, we investigated the evolution of the electronic states and spectral intensity transfer at the M point near the BZ boundary. Figures 3(a)–3(f) show snapshots of the dispersion images measured at different delay times in the M-Γ-M direction. Two main features were observed. First, the intensity of the folded Se_{4p} band decreased as a function of delay time. This is indicative of CDW melting and is also associated with the closing gap. This transiently excited state could be resolved more clearly in the differential images shown in Fig. 3(g). To understand the dynamics of the decreasing Se_{4p} bands, the temporal evolution of the folded Se_{4p} band around the M point, which has a lifetime of 3.0 ± 0.6 ps,

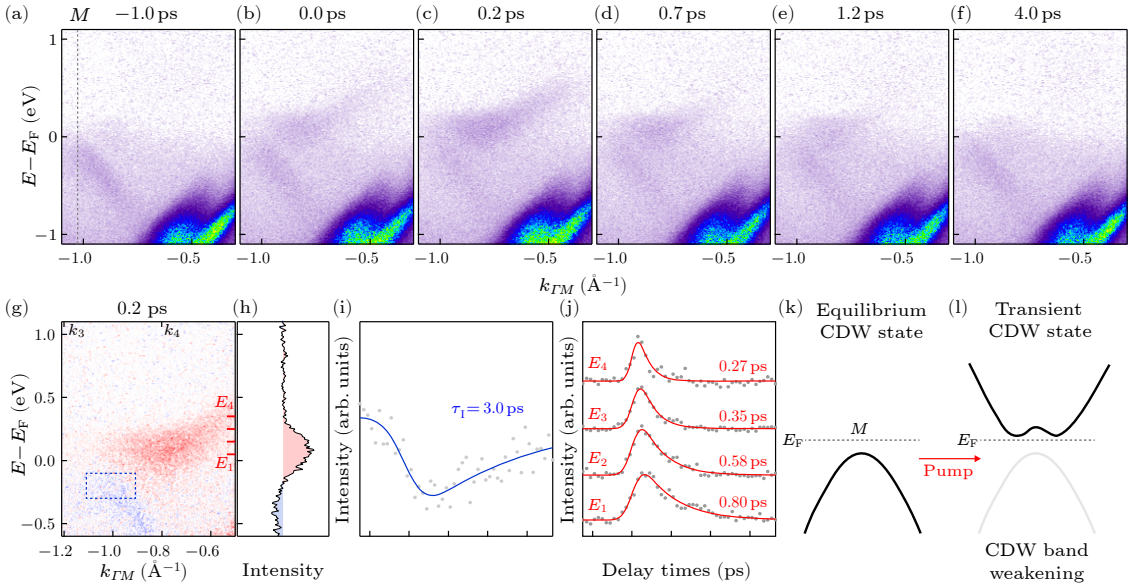

Fig. 3. Light-induced dynamics and spectral weight distribution near the BZ border. (a)–(f) TrARPES dispersion images at different delay times around point M in the M-Γ-M direction. The pump photon energy is 1.2 eV and the pump fluence is 60 μJ/cm^2. The red arrows indicate the bottom of the conduction band below E_F. (g) Differential image obtained from the difference between the images shown in (c) and (a). (h) Integrated spectral weights from k_3 to k_4. (i) Intensity evolution of band weakening as a function of the delay time, which is obtained by integrating over the blue box marked in (g). (j) Intensity evolution extracted from points E_1 to E_4, which are marked in (g). (k) and (l) Schematics of the equilibrium CDW state before the pump and transient CDW state after the pump at point M. The pump induces CDW band weakening.

is shown in Fig. 3(i). This lifetime is comparable to the lifetime of the upshift at the Γ point, suggesting that this feature can also be regarded as a signature of CDW order melting. Second, the previously unoccupied Ti_{3d} band, marked by a blue line in Fig. 1(c), was filled by electron injection from the Se_{4p} band via photo-excitation. This explains the decrease in the spectral weight from the Γ point at the same momentum (Supplementary Information Fig. S4). As a confirmation of this phenomenon, the integral of the spectral intensity from k_3 to k_4 at $\Delta t = 0.2$ ps [see Fig. 3(g)], shows an increasing spectral weight. To understand the relaxation dynamics of the Ti_{3d} band, in Fig. 3(j), we plot the temporal intensity evolution from E_1 to E_4. These points (E_1 to E_4) are marked in Fig. 3(g). The fast relaxation time (less than 1 ps) suggests relaxation through electron–phonon interactions.[31,47] The CDW melting and carrier dynamics are summarized in Figs. 3(k) and 3(l), which show that the folded Se_{4p} bands are weakened owing to CDW melting, and the Ti_{3d} band is filled owing to photo-excitation.

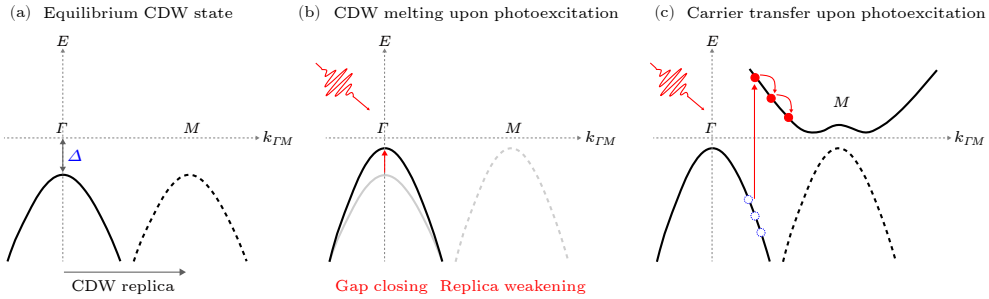

Fig. 4. Schematic of the complete dynamics covering the first BZ before and after photo-excitation. (a) Schematic of CDW phase induced band-folding in momentum image. (b) Schematic of CDW melting under photo-excitation. (c) Schematic of carrier transfer upon photo-excitation.

To obtain a complete picture of the photoexcited carriers, the global dynamics at all momenta at different stages before and after photo-excitation are shown in Fig. 4. In the equilibrium CDW phase without pumping, folded Se_{4p} bands appeared at the M point owing to the new periodicity of the commensurate CDW in real space [indicated by the black dashed lines in Fig. 4(a)]. Upon photo-excitation, the Se_{4p} valence band at the BZ center shifted upward, leading to gap closing in CDW. Meanwhile, the replica of the Se_{4p} bands weakened [see the schematic in Fig. 4(b)]. Both features suggest photoinduced CDW melting. Moreover, a spectral intensity transfer occurred from the BZ center to the BZ boundary; that is, the carrier was excited from the Se_{4p} valence band to the Ti_{3d} conduction band and then relaxed into the bottom of the band minimum through electron-phonon scattering [see the schematic in Fig. 4(c)]. These dynamics reveal the important role of light pulses in the exploration and manipulation of solids.

4. Conclusion. In summary, XUV TrARPES measurements on 1T-$TiSe_2$ allowed us to obtain the global scope of CDW melting-induced spectral intensity distribution dynamics covering the entire BZ. CDW melting was studied with respect to two aspects: gap closing of CDW and weakening of the CDW folded band. Our work provides comprehensive spectroscopic evidence of ultrafast carrier dynamics across the entire BZ. We envision that such tunable long-range order and transiently populated electronic states may provide more possibilities for optical manipulation in real and momentum spaces.

Acknowledgment. This study was supported by the Synergetic Extreme-Condition User Facility (SECUF), the National Key R&D Program of China (Grant Nos. 2021YFA1400100, 2020YFA0308800, and 2022YFA1604200), and the National Natural Science Foundation of China (Grant Nos. 12234011, 92250305, 52388201, 11725418, and 11427903). C.B. was supported by the China Postdoctoral Science Foundation (Grant Nos. 2022M721886 and BX20230187) and the Shuimu Tsinghua Scholar Program.

References

[1] Wang Y H, Steinberg H, Jarillo-Herrero P, and Gedik N 2013 *Science* **342** 453
[2] Mahmood F, Chan C K, Alpichshev Z, Gardner D, Lee Y, Lee P A, and Gedik N 2016 *Nat. Phys.* **12** 306
[3] Zhou S, Bao C, Fan B, Zhou H, Gao Q, Zhong H, Lin T, Liu H, Yu P, Tang P, Meng S, Duan W, and Zhou S 2023 *Nature* **614** 75
[4] Zhou S, Bao C, Fan B, Wang F, Zhong H, Zhang H, Tang P, Duan W, and Zhou S 2023 *Phys. Rev. Lett.* **131** 116401
[5] Ito S, Schüler M, Meierhofer M, Schlauderer S, Freudenstein J, Reimann J, Afanasiev D, Kokh K A, Tereshchenko O E, Güdde J, Sentef M A, Höfer U, and Huber R 2023 *Nature* **616** 696
[6] Fausti D, Tobey R I, Dean N, Kaiser S, Dienst A, Hoffmann M C, Pyon S, Takayama T, Takagi H, and Cavalleri A 2011 *Science* **331** 189
[7] Mitrano M, Cantaluppi A, Nicoletti D, Kaiser S, Perucchi A, Lupi S, Di Pietro P, Pontiroli D, Riccò M, Clark S R, Jaksch D, and Cavalleri A 2016 *Nature* **530** 461
[8] Stojchevska L, Vaskivskyi I, Mertelj T, Kusar P, Svetin D, Brazovskii S, and Mihailovic D 2014 *Science* **344** 177
[9] Morrison V R, Chatelain R P, Tiwari K L, Hendaoui A, Bruhács A, Chaker M, and Siwick B J 2014 *Science* **346** 445
[10] Kogar A, Zong A, Dolgirev P E, Shen X Z, Straquadine J, Bie Y Q, Wang X R, Rohwer T, Tung I C, Yang Y F, Li R K, Yang J, Weathersby S, Park S, Kozina M E, Sie E J, Wen H D, Jarillo-Herrero P, Fisher I R, Wang X J, and Gedik N 2020 *Nat. Phys.* **16** 159

[11] Li X, Qiu T, Zhang J, Baldini E, Lu J, Rappe A M, and Nelson K A 2019 *Science* **364** 1079

[12] Wandel S, Boschini F, da Silva Neto E H, Shen L, Na M X, Zohar S, Wang Y, Welch S B, Seaberg M H, Koralek J D, Dakovski G L, Hettel W, Lin M F, Moeller S P, Schlotter W F, Reid A H, Minitti M P, Boyle T, He F, Sutarto R, Liang R, Bonn D, Hardy W, Kaindl R A, Hawthorn D G, Lee J S, Kemper A F, Damascelli A, Giannetti C, Turner J J, and Coslovich G 2022 *Science* **376** 860

[13] Lian C, Zhang S J, Hu S Q, Guan M X, and Meng S 2020 *Nat. Commun.* **11** 43

[14] Trigo M, Giraldo-Gallo P, Clark J N, Kozina M E, Henighan T, Jiang M P, Chollet M, Fisher I R, Glownia J M, Katayama T, Kirchmann P S, Leuenberger D, Liu H, Reis D A, Shen Z X, and Zhu D 2021 *Phys. Rev. B* **103** 054109

[15] Yusupov R, Mertelj T, Kabanov V V, Brazovskii S, Kusar P, Chu J H, Fisher I R, and Mihailovic D 2010 *Nat. Phys.* **6** 681

[16] Huber T, Mariager S O, Ferrer A, Schäfer H, Johnson J A, Grübel S, Lübcke A, Huber L, Kubacka T, Dornes C, Laulhe C, Ravy S, Ingold G, Beaud P, Demsar J, and Johnson S L 2014 *Phys. Rev. Lett.* **113** 026401

[17] Wang R, Ding J, Sun F, Zhao J, and Qiu X 2024 *Chin. Phys. Lett.* **41** 057801

[18] Di Salvo F J, Moncton D E, and Waszczak J V 1976 *Phys. Rev. B* **14** 4321

[19] Kogar A, Rak M S, Vig S, Husain A A, Flicker F, Joe Y I, Venema L, MacDougall G J, Chiang T C, Fradkin E, van Wezel J, and Abbamonte P 2017 *Science* **358** 1314

[20] Monney C, Cercellier H, Clerc F, Battaglia C, Schwier E, Didiot C, Garnier M G, Beck H, Aebi P, Berger H, Forró L, and Patthey L 2009 *Phys. Rev. B* **79** 045116

[21] Kidd T E, Miller T, Chou M Y, and Chiang T C 2002 *Phys. Rev. Lett.* **88** 226402

[22] Zhu L, Zhao W M, Jia Z Y, Li H P, Xie X D, Li Q Y, Wang Q W, Dou L G, Hu J G, Zhang Y, Zhu W G, Yu S L, Li J X, and Li S C 2023 *Chin. Phys. Lett.* **40** 057101

[23] Weber F, Rosenkranz S, Castellan J P, Osborn R, Karapetrov G, Hott R, Heid R, Bohnen K P, and Alatas A 2011 *Phys. Rev. Lett.* **107** 266401

[24] Otto M R, Pöhls J H, René de Cotret L P, Stern M J, Sutton M, and Siwick B J 2021 *Sci. Adv.* **7** eabf2810

[25] Hellgren M, Baima J, Bianco R, Calandra M, Mauri F, and Wirtz L 2017 *Phys. Rev. Lett.* **119** 176401

[26] Boschini F, Zonno M, and Damascelli A 2024 *Rev. Mod. Phys.* **96** 015003

[27] Bao C, Tang P, Sun D, and Zhou S 2022 *Nat. Rev. Phys.* **4** 33

[28] Zhang H, Pincelli T, Jozwiak C, Kondo T, Ernstorfer R, Sato T, and Zhou S 2022 *Nat. Rev. Methods Primers* **2** 54

[29] Rohwer T, Hellmann S, Wiesenmayer M, Sohrt C, Stange A, Slomski B, Carr A, Liu Y W, Avila L M, Kalläne M, Mathias S, Kipp L, Rossnagel K, and Bauer M 2011 *Nature* **471** 490

[30] Monney C, Puppin M, Nicholson C W, Hoesch M, Chapman R T, Springate E, Berger H, Magrez A, Cacho C, Ernstorfer R, and Wolf M 2016 *Phys. Rev. B* **94** 165165

[31] Hedayat H, Sayers C J, Bugini D, Dallera C, Wolverson D, Batten T, Karbassi S, Friedemann S, Cerullo G, van Wezel J, Clark S R, Carpene E, and Da Como E 2019 *Phys. Rev. Res.* **1** 023029

[32] Hedayat H, Sayers C J, Ceraso A, van Wezel J, Clark S R, Dallera C, Cerullo G, Da Como E, and Carpene E 2021 *New J. Phys.* **23** 033025

[33] Duan S, Xia W, Huang C, Wang S, Gu L, Liu H, Xiang D, Qian D, Guo Y, and Zhang W 2023 *Phys. Rev. Lett.* **130** 226501

[34] Duan S, Cheng Y, Xia W, Yang Y, Xu C, Qi F, Huang C, Tang T, Guo Y, Luo W, Qian D, Xiang D, Zhang J, and Zhang W 2021 *Nature* **595** 239

[35] Mathias S, Eich S, Urbancic J, Michael S, Carr A V, Emmerich S, Stange A, Popmintchev T, Rohwer T, Wiesenmayer M, Ruffing A, Jakobs S, Hellmann S, Matyba P, Chen C, Kipp L, Bauer M, Kapteyn H C, Schneider H C, Rossnagel K, Murnane M M, and Aeschlimann M 2016 *Nat. Commun.* **7** 12902

[36] Huber M, Lin Y, Dale N, Sailus R, Tongay S, Kaindl R A, and Lanzara A 2022 *J. Phys. Chem. Solids.* **168** 110740

[37] Huber M, Lin Y, Dale N, Sailus R, Tongay S, Kaindl R A, and Lanzara A 2022 *Sci. Rep.* **12** 15860

[38] Huber M, Lin Y, Marini G, Moreschini L, Jozwiak C, Bostwick A, Calandra M, and Lanzara A 2024 *Sci. Adv.* **10** eadl4481

[39] Teng H, Zhong S, He X, Zhao K, Yun C, Dong S, and Wei Z 2024 *Acta Opt. Sin.* **44** 1732016

[40] Chen F, Wang J, Pan M, Liu J, Huang J, Zhao K, Yun C, Qian T, Wei Z, and Ding H 2023 *Rev. Sci. Instrum.* **94** 043905

[41] Cercellier H, Monney C, Clerc F, Battaglia C, Despont L, Garnier M G, Beck H, Aebi P, Patthey L, Berger H, and Forró L 2023 *Opt. Express* **31** 9854

[42] Cercellier H, Monney C, Clerc F, Battaglia C, Despont L, Garnier M, Beck H, Aebi P, Patthey L, Berger H, and Forró 2007 *Phys. Rev. Lett.* **99** 146403

[43] Möhr-Vorobeva E, Johnson S L, Beaud P, Staub U, De Souza R, Milne C, Ingold G, Demsar J, Schaefer H, and Titov A 2011 *Phys. Rev. Lett.* **107** 036403

[44] Bao C, Luo L, Zhang H, Zhou S, Ren Z, and Zhou S 2021 *Rev. Sci. Instrum.* **92** 033904

[45] Zhong H, Bao C, Lin T, Zhou S, and Zhou S 2022 *Rev. Sci. Instrum.* **93** 113910

[46] Bao C, Zhong H, Zhou S, Feng R, Wang Y, and Zhou S 2022 *Rev. Sci. Instrum.* **93** 013902

[47] Hellmann S, Rohwer T, Kalläne M, Hanff K, Sohrt C, Stange A, Carr A, Murnane M M, Kapteyn H C, Kipp L, Bauer M, and Rossnagel K 2012 *Nat. Commun.* **3** 1069